Mode-Field Diameter and "Spot Size" Measurements of Lensed and Tapered Specialty Fibers

Jeffrey L. Guttman
PHOTON, inc., 6860 Santa Teresa Blvd., San Jose, CA 95119
Phone: 408-226-1000, FAX: 408-226-1025, e-mail: jguttman@photon-inc.com

Abstract: The Mode-Field Diameter (MFD) and "spot size" of an assortment of lensed and tapered specialty fibers were determined from far-field and near-field measurements. In the far field, measurements were made using a 3D-scanning goniometric radiometer that provides a complete hemispherical profile. Indirect measures of the near field derived from these data are reported, including the Petermann II MFD, the $1/e^2$ spot size using the far-field Gaussian approximation, and a measure obtained from 2D Fourier transform inversion of the far field using phase retrieval techniques. In the near field, direct profile measurements were made using an IR Vidicon camera and magnifying objective lenses, with the spot size reported as the $1/e^2$ diameter of the imaged profile.

1. Introduction

Lensed and Tapered specialty fibers are designed to optimize coupling between the fiber and various optical components such as edge-emitting laser diodes and AWGs. The light from these fibers forms a focus at some finite distance away from the fiber end. The MFD and corresponding spot size of these fibers is typically in the range of 5 microns or less. These small spot sizes and corresponding high divergence present challenges to near field and far field measurements. Typically the near-field measurements are limited by the optical performance, and the far-field measures must extend to very large angles. Results of measurements of 6 commercially available fibers are presented, including different type lensed/tapered fibers (4 axially symmetric and 1 elliptical) and a standard single-mode fiber for reference. Also, since the focused beams are in free space, there are some fundamental questions as to the applicability of the MFD, a measure originally formulated to describe the field distribution within a fiber.

2. Measurement Technique

The fibers were coupled to a stable narrow-linewidth diode laser source operating at a nominal wavelength of 1550 nm and output power of approximately 7dBm.

Far-field profiles were obtained using a 3D scanning goniometric radiometer, with optical dynamic range greater than 60 dB. This instrument provides NIST-traceable measures of MFD to the 0.5% level for single-mode fiber. The angular measurement range for each scan is ±90°, with sampling every 0.055°. By rotating the source about the scan plane, a full hemispherical measure of the far-field profile is obtained. The 3D profiles for each fiber in this study consist of 50 azimuthal scans at increments of 3.6° about the fiber axis.

Near-field profile measurements were made using an IR Vidicon camera and 2 different magnifying objective lenses: a 100X NA 0.9 microscope objective intended for use in the visible and a 40X NA 0.48 aspheric lens designed for the IR. The point-spread function of this lens at 1550 nm is approximately 2.6 µm. The characteristics of the 100X lens at 1550nm are not known. The fibers were positioned using a high precision 3-axis translation stage. Absorbing glass filters were used for optical attenuation. The RS-170 camera video images were acquired using a framegrabber with 8-bit resolution, i.e., 256 levels. Measurement accuracy depends on the camera noise, sensor response uniformity, the digitization, the number of pixels in the image, and on the optical properties of the lens used. With adequate pixel count and lens quality, the signal noise and sensor response provide accuracy to the ±3% level. Accuracy is also strongly dependent on the lens position because of the short depth of focus of both the lens and the fibers being measured.

3. Measurement Results

Complete hemispherical far-field profiles of the 6 fibers, (designated fibers # 1-6), and the corresponding 1D cross-sectional profiles through the principal axes of the distribution, are shown in figure 1. The background level of the measurements, seen in figure 1a for the profile of the standard single-mode fiber, is at the -60dB level relative to the peak. The profiles of the lensed/tapered fibers extend in all cases to ±90°. The profiles for fibers #1-5 have the appearance of a superposition of a main beam and a scatter background, probably due to surface modifications and defects introduced in the fabrication process. The angular extent of the main beam for these profiles ranges from approximately ±30° for the standard single-mode fiber to greater than ±70° for fiber #5. The profile for fiber #6, the elliptical fiber, consists of a main beam with a prominent diffraction structure. (Although not shown here, the scatter and diffraction structure extend to angles greater than ±90°, in the backward direction.)

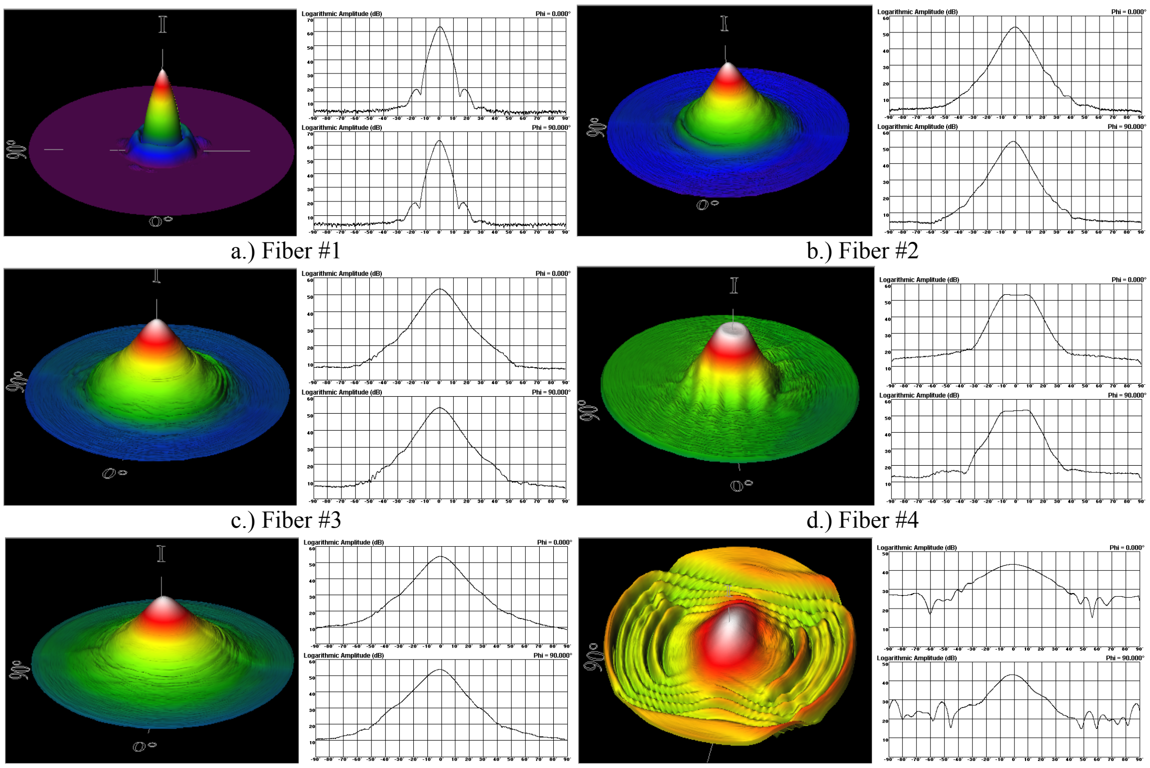

a.) Fiber #1 b.) Fiber #2

c.) Fiber #3 d.) Fiber #4

e.) Fiber #5 f.) Fiber #6

Figure 1. Complete hemispherical far field profiles of fibers # 1-6, and the corresponding 1D cross-sectional profiles through the principal axes of the distribution. The vertical scale is 10dB/division and the horizontal scale is 10°/division.

Example images obtained in the near field for fiber #6, the elliptical fiber with the smallest spot size of all the fibers measured here, are shown in figure 2. The profile in figure 2a obtained with the 40X lens is clearly seen to be broadened by the spread function of the lens, and is also near the limit of adequate pixel count.

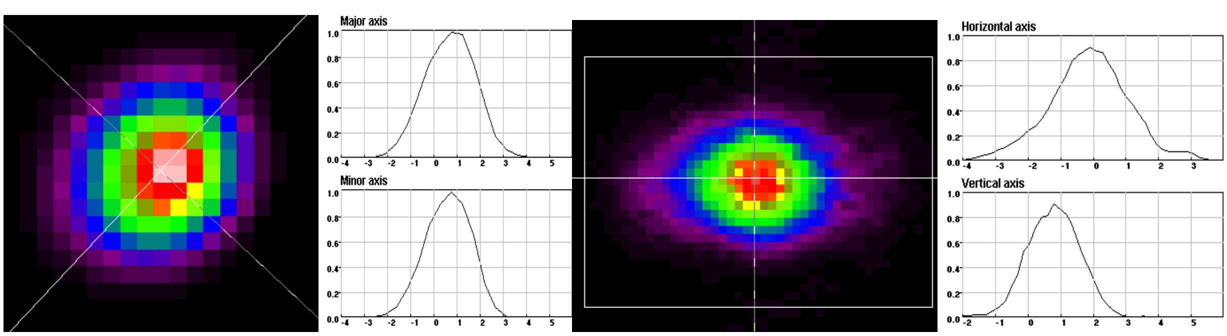

a.) 40X b.) 100X

Figure 2. Near field profiles of fiber #6, the elliptical lensed/tapered fiber, obtained with a.) 40X lens and b.) 100X lens. The horizontal scale in the profile cross sections is 1 µm/division.

4. Analysis and Discussion

The far field data were analyzed to provide the Petermann II MFD [1], the $1/e^2$ diameter from a diffraction-limited Gaussian approximation using the ISO/DIS 13694 laser standard fit [2], and the $1/e^2$ diameter of the near field obtained from 2D Fourier analysis with phase retrieval [3-5]. The near field profile data were analyzed to provide the $1/e^2$ diameter, using the equivalent scanning slit method. The profile diameters obtained with the 40X lens were corrected for the spread function width.

The MFD for the lensed/tapered fibers depends significantly on the angular integration limit of the Petermann II integral, due to the wide angular extent of the far field. This is shown in the graph of MFD versus the Petermann II integral limit shown in figure 3. The MFD stabilizes for most of the fibers in the range from 40° to 60°. For the elliptical fiber #6 the integration needs to extend beyond 70°. However, the Petermann II formulation has radial symmetry as an underlying assumption. Therefore, strictly speaking, it is inappropriate to use this MFD measure for elliptical fibers. Table 1 summarizes the MFD results over the integral limit ranging from 40° to 60°. The fractional percent variation from the average value for fibers #1-5 is well within acceptable limits, and errors associated with the elliptical fiber are quite significant.

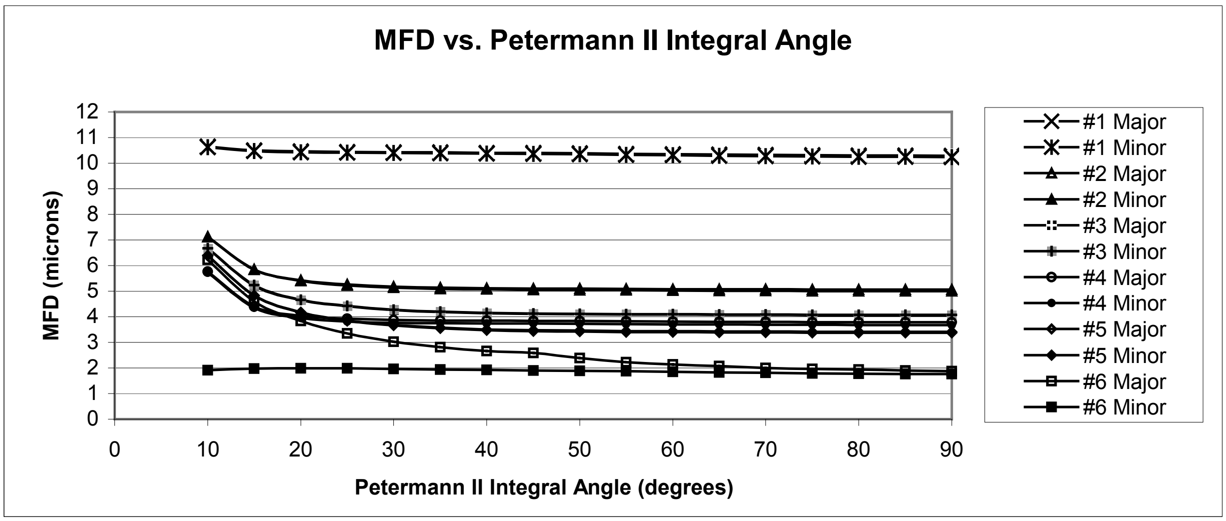

Figure 3. MFD vs. Petermann II integration limit for fibers #1-6.

Table 1. Mode-Field Diameter for Various Angular Limits of the Petermann II Integral

	Mode-Field Diameter (μm)											
Fiber	1		2		3		4		5		6	
Integral Limit	Major and Minor Axes											
40	10.406	10.375	5.069	5.118	4.141	4.154	3.851	3.742	3.478	3.506	2.668	1.920
45	10.395	10.361	5.054	5.104	4.113	4.128	3.842	3.734	3.442	3.476	2.593	1.902
50	10.382	10.345	5.043	5.095	4.100	4.110	3.832	3.725	3.420	3.457	2.391	1.887
55	10.367	10.328	5.034	5.087	4.091	4.100	3.823	3.715	3.405	3.443	2.221	1.873
60	10.352	10.311	5.026	5.081	4.084	4.094	3.814	3.705	3.395	3.434	2.139	1.851
Average	10.380	10.344	5.045	5.097	4.106	4.117	3.832	3.724	3.428	3.463	2.402	1.887
	Difference from Average MFD											
40	0.2%	0.3%	0.5%	0.4%	0.9%	0.9%	0.5%	0.5%	1.5%	1.2%	11.1%	1.8%
45	0.1%	0.2%	0.2%	0.1%	0.2%	0.3%	0.3%	0.3%	0.4%	0.4%	7.9%	0.8%
50	0.0%	0.0%	0.0%	0.0%	-0.1%	-0.2%	0.0%	0.0%	-0.2%	-0.2%	-0.5%	0.0%
55	-0.1%	-0.2%	-0.2%	-0.2%	-0.4%	-0.4%	-0.2%	-0.2%	-0.7%	-0.6%	-7.6%	-0.7%
60	-0.3%	-0.3%	-0.4%	-0.3%	-0.5%	-0.6%	-0.5%	-0.5%	-1.0%	-0.8%	-11.0%	-1.9%

The $1/e^2$ diameter spot sizes obtained from the far and near field analyses are summarized in Table 2. For any fiber, the diameter reported using the different methods varies significantly, on the order of ±15-20%. This result is not surprising for these sources. The extremely non-Gaussian shape of the far field makes the Gaussian approximation highly questionable. Similarly, the very small spot size of the lensed/tapered fibers is at or beyond the performance limits of the optical near-field imaging techniques, and the measured values must undergo significant corrections that increase uncertainty and error. The most accurate method here may be that of the 2D Fourier transform with phase retrieval. It is also observed that these values are overall the most consistent with the MFD values.

Table 2. Near Field $1/e^2$ Diameter Spot Size from Near Field and Far Field Data

	$1/e^2$ Diameter (μm)					
Fiber	1	2	3	4	5	6
Method of Analysis	Major Axis × Minor Axis					
$1/e^2$ FF Gaussian	11.77×11.77	6.20×6.16	5.07×5.11	3.64×3.51	4.23×4.25	3.62×2.07
$1/e^2$ NF Profile 100X	10.29×9.71	4.67×4.67	4.37×4.29	4.23×4.09	3.50×3.36	3.58×2.34
$1/e^2$ NF Profile 40X	9.24×9.03	4.85×4.73	4.24 ×4.15	3.79×3.55	4.03×3.79	3.55×2.77
2D FF Fourier Transform	9.94×9.93	5.04×5.03	4.02×4.07	3.60×3.55	3.71×3.30	2.96×1.94

5. Conclusion

Lensed and tapered specialty fibers exhibit wide angular divergence and corresponding small spot sizes. These characteristics pose significant challenges to measurement of MFD and spot size. The results presented highlight the limitations of standard near-field optical techniques, and the necessity for far-field measurements to include very wide angles. Specifically, for some of the fibers measured here, far-field measurement instruments must acquire data at angles extending to ±60° or greater for accurate determination of the MFD. For near-field measurements using conventional optical techniques, the small spot sizes of these fibers push the limits of resolution and can lead to significant errors. Also, the typically non-Gaussian profiles of lensed and tapered fibers also lend doubts as to the accuracy of Gaussian approximations used to determine spot size. Estimation of spot size using these methods shows considerable variation. Due to this, and also to ease of measurement, far-field transform techniques are the preferred method of characterization.

For radially symmetric fibers, specification of the Petermann II MFD to characterize the focused beam yields consistent results and appears to be fine, but due to variation in the integral with angular limit and to avoid ambiguity, the actual limit used in the calculation should be specified as well as the MFD value. For non-radially symmetric fibers, use of the Petermann II MFD, although it does provide a measure, is problematic and highly questionable based on the underlying assumptions of radial symmetry in the Petermann II integral. For such non-radially symmetric fibers, the development of new metrics using 2D Fourier transform methods may provide more accurate and consistent specifications.

6. Acknowledgements

The author is grateful to David Pikey for his efforts in the implementation of the algorithm for the 2D Fourier transform with phase retrieval.

7. References

1. "Measurement of Mode-Field Diameter of Single-Mode Optical Fiber", Fiberoptic Test Procedure FOTP-191, Telecommunications Industry Association, Standards and Technology Department, 2500 Wilson Blvd., Suite 300, Arlington, VA, 22201 (1998).
2. ISO/DIS Standard 13694, "Test methods for laser beam power (energy) density distribution", International Organization for Standardization, September 1998.
3.J.R.Fienup, "Reconstruction of an Object from the modulus of its Fourier transform", Optics Letters, Vol. 3, No. 1, pp 27-29, July 1978.
4. J.R.Fienup, "Phase retrieval algorithms: a comparison", Applied Optics, Vol. 21, No. 15, pp. 2758-2769, August 1982.
5. J.R.Fienup and C.C.Wackermann, "Phase retrieval stagnation problems and solutions", J. Opt. Soc. Am. A, Vol. 3, No.11, pp. 1897-1907, November 1986.